Mathematical Biology and Bioinformatics
2022. V. 17. № 2. P. 338–359. doi: 10.17537/2022.17.338

========== **BIOINFORMATICS** ==========

Identification of Novel miRNAs Involved in Cancer Progression and Metastasis in Clear Cell Renal Cell Carcinoma

Rana Hazim Hamoode[1], Tamadher Abbas Rafaa[2], Rafat Hamdi Abduljaleel[3], Ahmed AbdulJabbar Suleiman[3*]

[1]*College of Dentistry, University of Anbar, Ramadi, Anbar, Iraq*
[2]*The Presidency of the University of Anbar, Ramadi, Anbar, Iraq*
[3]*Department of Biotechnology, College of Science, University of Anbar, Ramadi, Anbar, Iraq*

Abstract. Cancer cells alter the metabolic pathways that are feasible for their growth and development. Clear cell renal cell carcinoma, which is characterized by loss or mutation of VHL gene, which promotes cell invasiveness. The global incidence rate of kidney cancer was 319,016 in 2020. MicroRNAs are 21–23nt long, conserved and non-coding molecules, involved in gene expression regulation by RNA silencing and post-transcriptional gene regulation. It has been reported that microRNA dysregulation is associated with clear cell renal cell carcinoma along with various human cancers such as breast cancer, colorectal cancer, ovarian cancer and hepatocellular carcinoma. However, the aim of this study was to identify microRNAs that are differentially expressed between normal kidney tissue and clear cell renal cell carcinoma samples. For this research, a publicly available microRNA dataset was retrieved from ArrayExpress, followed by preprocessing. Mapping, identification of known and novel microRNAs, and quantification were executed using miRDeep2 to perform differential expression analysis using DESeq R/Bioconductor package. Target identification and functional enrichment analysis were conducted using GeneCodis4. In total 2656 microRNAs were found to be differentially expressed, among which upregulated and downregulated microRNAs were 229 and 302 respectively. This study identifies five microRNAs that were significantly related to clear cell renal cell carcinoma, along with a novel set of five microRNAs that have not been investigated previously for clear cell renal cell carcinoma.

Key words: *KC, ccRCC, miRNA, DEA, DE, EMT, EGFR, GO.*

INTRODUCTION

Kidney cancer (KC), also termed as renal cancer, is a metabolic disease which encompasses different types of cancer [1]. Each type of cancer is caused by a different gene with different responses to therapies [2]. The cells in the kidney become cancerous and grow out of control. Almost 90 % of KCs start in the lining of tiny tubules. These tubules function as a filter that cleans waste substances from blood and returns the required materials [3]. The exact cause of KC is unknown but multiple factors can contribute to its incidence such as high BP, long-term dialysis, older age and family history of KC [4]. According to GLOBOCAN 2020 global cancer statistics, the estimated incidence rate of kidney cancer was 319,016 worldwide. The KC incidence rate has been reported higher in Asia with a percentage of 37.6 % cases, followed by Europe with 31.2 % cases [5].

[*]Corresponding author: Ahmed A. Suleiman (ORCID ID: 0000-0001-7427-4483)
e-mail: ahmed.suleiman@uoanbar.edu.iq

There are multiple types of KCs based on the location of their occurrence in kidneys such as wilms tumor, renal sarcoma, urothelial carcinoma, renal lymphoma and acute renal failure. Renal cell carcinoma (RCC), a prevalent type of KC, develops in the proximal renal tubules. These tubules function in filtering the nutrients and return them back to blood. One of the predominant type of RCC is, Clear cell renal cell carcinoma (ccRCC) [6]. It characterizes the disruption of the VHL gene that encodes for pVHL. This protein is crucial for exposing transcription factors that are involved in response to hypoxia. Absence of pVHL disrupts glycolysis, angiogenesis and lipolysis. Loss of VHL also promotes cell invasiveness, a phenomenon important in tissue development. But increase in cell invasiveness leads to onset of RCC [7].

Micro RNA (miRNA), a small non-coding RNA (21–23 nt), involves in RNA silencing and post transcriptional gene regulation. It functions by suppressing the target expression through translational inhibition or mRNA destabilization [8]. MiRNAs suppress cellular processes such as cell migration, differentiation, cell cycle regulation and apoptosis by regulating genes performing these processes. It has been reported that overexpression of miRNA results in diverse human cancers such as b-cell lymphomas, lung cancer and renal cancer and functions as tumor suppressor or oncogenes [9]. According to published reports, upregulation of adhesion molecules such as cell adhesion molecule M2 (CADM2) results in tumor suppression and inhibition of ccRCC metastasis. But overexpression of certain miRNAs for example miRNA-146a counteract these functions by promoting cell proliferation and tumor growth [10]. Studying miRNAs is crucial as it helps to recognize the potential targets such as CADM2 that are suppressed in tumor progression [11].

Differential expression analysis (DEA) enables us to identify quantitative changes in expression levels across experimental conditions by applying statistical analysis [12]. In this study, we have identified miRNAs that are differentially expressed (DE) in ccRCC individuals as compared to normal, using integrative pathway analysis approach. These DE miRNAs will provide further insights in identifying targets that are suppressed due to miRNA binding. Moreover, the disrupted functional roles of miRNAs involved in essential metabolic and signaling pathways are also identified which may result in ccRCC development and progression.

MATERIALS AND METHODS

The overall workflow of this study includes the preprocessing of the miRNA datasets followed by their mapping on the reference genome. Then the mapped reads were quantified followed by miRNA DEA. The miRNA-mRNA targets were predicted using different databases to identify the target genes that are deregulated by miRNAs in ccRCC.

Data collection

The selection criteria that was applied to obtain the datasets was that the dataset must be from the origin of *Homo sapiens* and not from a cell-line study. Moreover, the samples were taken from the renal tumor tissues from the patients. For the analysis, miRNA dataset E-GEOD-24457 was selected and retrieved from ArrayExpress database. The dataset is based on the above criteria and consists of 20 samples including 10 renal tumor and 10 normal renal samples.

Data preprocessing and mapping

Preprocessing and quality assessment of datasets is an important step for analysis because it ensures the quality of data being analyzed. FastQC (v0.11.9) software was used with default parameters to assess the quality of the raw data [13]. To trim the reads containing low-quality adapters and primers, fastp (v0.20.1) was used [14]. The trimming of PCR primers indicated by FastQC in overrepresented sequences, a FASTA file containing the primer sequences was

used as input for fastp. Filtered reads were generated with the following options: -w 14 --adapter_fasta –i, in which '–w' denotes number of threads (based on cpu cores), '–adapter_fasta' represents the FASTA file containing primer sequences and '-i' indicates the file containing raw reads. The filtered reads were then again assessed by FastQC to generate quality reports for individual samples.

Mapping of trimmed reads against the reference genome of Homo sapiens (GRCh38) was performed using the perl script (mapper.pl) of miRDeep2 (v0.0.7) package [15]. The mapper.pl script was implemented with a configuration file containing the accession number of all samples in a dataset, reference genome and trimmed reads. The script was executed with the following parameters: '-o' (denotes the cpu cores), '-e' (specifies that input file is in fastq format), '-u' (specifies to not remove directory with temporary files), '-h' (represents that file containing raw reads is converted to FASTA format), '-m' (indicates collapsed reads), '-p' (denotes map to genome), '-s' (specifies the file containing processed reads), '-t' (denotes a file containing read mappings), '-v' (outputs progress report). This results in generation of counts, source and genomic location of the mapped reads.

Novel miRNAs and quantification

The miRDeep2 was then used to find the novel and known miRNAs using the Perl script miRDeep2.pl. The script accepted the collapsed reads, reference genome, miRNA hairpin and mature miRNA FASTA sequences as input. These miRNA sequences were retrieved from miRBase database and the collapsed reads were generated by the mapping function [16]. Furthermore the quantification of expressed novel and known miRNAs was performed by miRDeep2 'quantifier.pl' script applying the parameters –p, -m, -r, -k.

Differential expression analysis of miRNA

For DE analysis between ccRCC and normal samples, the quantification script miRDeep2.pl generated raw counts that were then supplied to the DESeq R/Bioconductor package (v1.36.0) for DEA [17]. Only those miRNA were considered for differential expression that had a read count > 1. The miRNAs having p-value < 0.05 and logFC > 1.5 were regarded as upregulated. Whereas the miRNAs that have p-value < 0.05 and logFC < –1.5 were regarded as downregulated.

Target identification and functional enrichment analysis

To identify target genes of DE miRNAs, GeneCodis4 was used to perform functional and pathway enrichment analysis [18]. Both up and down regulated DE miRNAs were analyzed separately. The following parameters were used; organism: Homo sapiens, input type: miRNAs, annotations: gene ontology (GO) biological processes (BP), molecular functions (MF), and cellular components (CC) and KEGG pathways.

RESULTS

Identification of differentially expressed miRNAs

DEA of miRNAs between ccRCC and normal kidney tissues identified 2656 DE miRNAs between ccRCC tissues and normal kidney tissues (see Supplementary Data). The miRNAs with p-value < 0.05 and logFC > 1.5 were regarded as biologically and statistically upregulated which can be seen on right side of plot, whereas the miRNAs that have p-value < 0.05 and logFC < –1.5 were regarded as biologically and statistically downregulated which can be seen on left side of plot (Fig. 1). Through DEA, a total of 229 miRNAs were identified to be upregulated and 302 were downregulated. The top 10 upregulated DE miRNAs include miR-140-5p, miR-126-3p, miR-28-5p, miR-20a-5p, miR-671-5p, miR-186-5p, miR-627-5p, miR-338-5p, miR-30e-3p and miR-148b-5p (Table 1). The top 10

downregulated DE miRNAs include miR-424-3p, miR-107, miR-23b-5p, miR-499a-5p, miR-23a-3p, miR-128-3p, miR-7977, miR-29c-3p, miR-5100 and miR-4454 (Table 2).

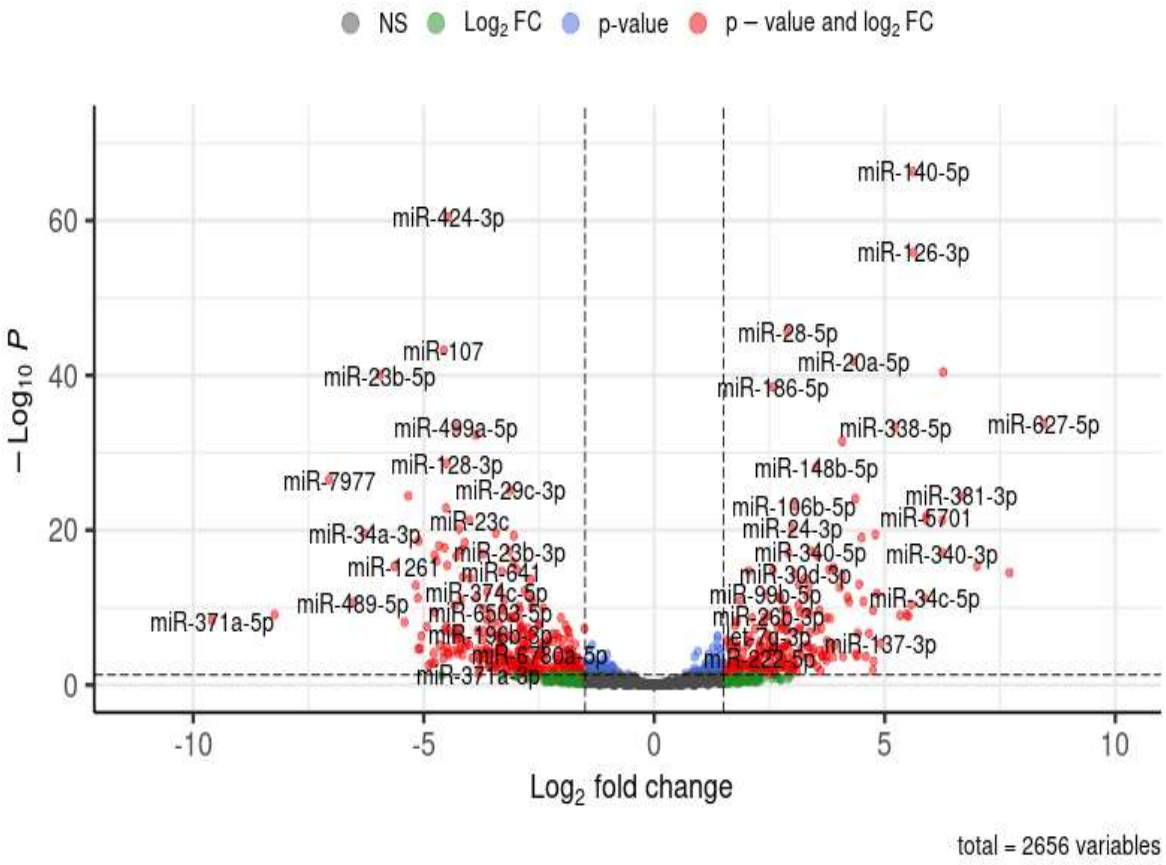

Fig. 1. Volcano plot for DE miRNAs. Red dots denote up (right) and down (left) regulated miRNAs that satisfy both p-value and log fold change criteria.

Table 1. Top 10 differentially expressed upregulated miRNAs

miRNA	log2FoldChange	*P*-value	Expression
hsa-miR-140-5p	5.612253312	4.88872E-67	UP
hsa-miR-126-3p	5.61375639	1.3006E-56	UP
hsa-miR-28-5p	2.88638036	2.26721E-46	UP
hsa-miR-20a-5p	4.323956821	1.34443E-42	UP
hsa-miR-671-5p	6.266454999	3.67931E-41	UP
hsa-miR-186-5p	2.580562291	3.05002E-39	UP
hsa-miR-627-5p	8.441878711	1.72938E-34	UP
hsa-miR-338-5p	5.224312237	4.49552E-34	UP
hsa-miR-30e-3p	4.077981328	3.33015E-32	UP
hsa-miR-148b-5p	3.514167426	7.74935E-29	UP

Table 2. Top 10 differentially expressed downregulated miRNAs

miRNA	log2FoldChange	*P*-value	Expression
hsa-miR-424-3p	–4.47683984052579	3.72195464741585E-61	DOWN
hsa-miR-107	–4.56520292971511	5.5248103769753E-44	DOWN
hsa-miR-23b-5p	–5.95164357592996	9.32979678736071E-41	DOWN
hsa-miR-499a-5p	–4.30643073610292	6.19834981755236E-34	DOWN
hsa-miR-23a-3p	–3.86905990881505	4.80853405680148E-33	DOWN
hsa-miR-128-3p	–4.50376327092788	2.26977682372693E-29	DOWN
hsa-miR-7977	–7.05724838455682	2.89562981694772E-27	DOWN
hsa-miR-29c-3p	–3.12747616185782	7.03057496255659E-26	DOWN
hsa-miR-5100	–5.33632951501035	3.76528338251652E-25	DOWN
hsa-miR-4454	–4.51517043387918	1.34994451445754E-23	DOWN

Gene ontology analysis

Both up and down regulated DE miRNAs were subjected to GO enrichment analysis. This analysis helps in determination of BP, MF and CC that might be impacted due to change in miRNA expression and subsequent dysregulation of genes. As indicated in Figure 2 and Table 3, the biological processes upregulated by DE miRNAs were primarily enriched in negative regulation of cell cycle G1/S phase transition (gene ratio: 41/114), positive regulation of cell death (gene ratio: 39/103), cellular response to amyloid-beta (gene ratio: 51/154), ubiquitin-dependent protein catabolic process (gene ratio: 38/105), autophagic cell death (gene ratio: 17/29) and cytoplasm sequestering of transcription factor (gene ratio: 11/17). These findings indicates that the upregulation of miRNA suppresses the genes involved in processes such as apoptosis, change in cellular activity, protein breakdown and cell death that results in cancer progression due to downregulation of subsequent genes. Whereas downregulated DE miRNAs were enriched in immune response (gene ratio: 51/210), cell-cell junction organization (gene ratio: 18/55), positive regulation of leukocyte adhesion to vascular endothelial cell (gene ratio: 18/55), regulation of modification of postsynaptic actin cytoskeleton (gene ratio: 8/16), DNA replication (gene ratio: 21/63), ossification involved in bone maturation (gene ratio: 9/18) and other processes that are involved in inflammatory response, cell proliferation and regulation of protein complexes are significantly related to tumorigenesis because of expression of genes involved in BP due to downregulation of miRNA (Figure 3, Table 4). Through molecular function enrichment of upregulated DE miRNAs (Figure 4, Table 5), tau protein kinase activity (gene ratio: 21/45), growth factor activity (gene ratio: 55/180), protein kinase binding (gene ratio: 93/369), transcription coregulator binding (gene ratio: 47/150) and DNA (cytosine-5-)-methyl transferase activity (gene ratio: 15/33) indicated that they may have cancer development and progression related functions because of dysregulation of proteins involved in cell growth and development. Alternatively, molecular function enrichment of downregulated DE miRNAs shows transforming growth factor beta receptor binding (gene ratio: 17/60), SUMO activating enzyme activity (gene ratio: 1/1), prostaglandin E receptor activity (gene ratio: 2/4), G rich

strand telomeric DNA binding (gene ratio: 3/7) and bicarbonate transmembrane transporter activity (gene ratio: 3/8) that indicates cancer progression and development by cell proliferation and membrane receptor disruption through regulation of gene by miRNA downregulation (Figure 5, Table 6). The upregulated DE miRNAs of cellular component (Figure 6, Table 7) were chiefly enriched in BIM-BCL-2 complex (gene ratio: 14/23), Cul4A-RING E3 ubiquitin ligase complex (gene ratio: 13/20), BIM-BCL-xl complex (gene ratio: 14/23), actin filament (gene ratio: 26/61), autophagosome (gene ratio: 22/52), microtubule (gene ratio: 34/104) and ubiquitin ligase complex (gene ratio: 23/55). This indicates disrupted apoptosis due to upregulated miRNA suppression that causes dysregulation of mitochondrial outer membrane permeabilization, which makes it unable to activate caspases that are primary effectors during apoptosis. In addition, the upregulation of miRNA results in initiation and progression of cancer because of unrepaired DNA damage due to dysregulated DNA repair and protein degradation. On contrary, the downregulated DE miRNAs of cellular components were mainly enriched in extracellular vesicles (gene ratio: 16/39), golgi lumen (gene ratio: 22/83), endoplasmic reticulum membrane (gene ratio: 57/258), cytosol (gene ratio: 116/576) and endoplasmic reticulum (ER) chaperone complex (gene ratio: 5/10) (Figure 7, Table 8). The results suggested that miRNA downregulation causes gene expression involved in delivering bioactive molecules to tumor and tumor associated cells. Furthermore this downregulation results in unfolded protein response (UPR) which is both apoptotic and adaptive in tumor cells. In addition, activation of ER chaperones that maintain ER homeostasis, contributes to cancer cell survival and progression in ccRCC.

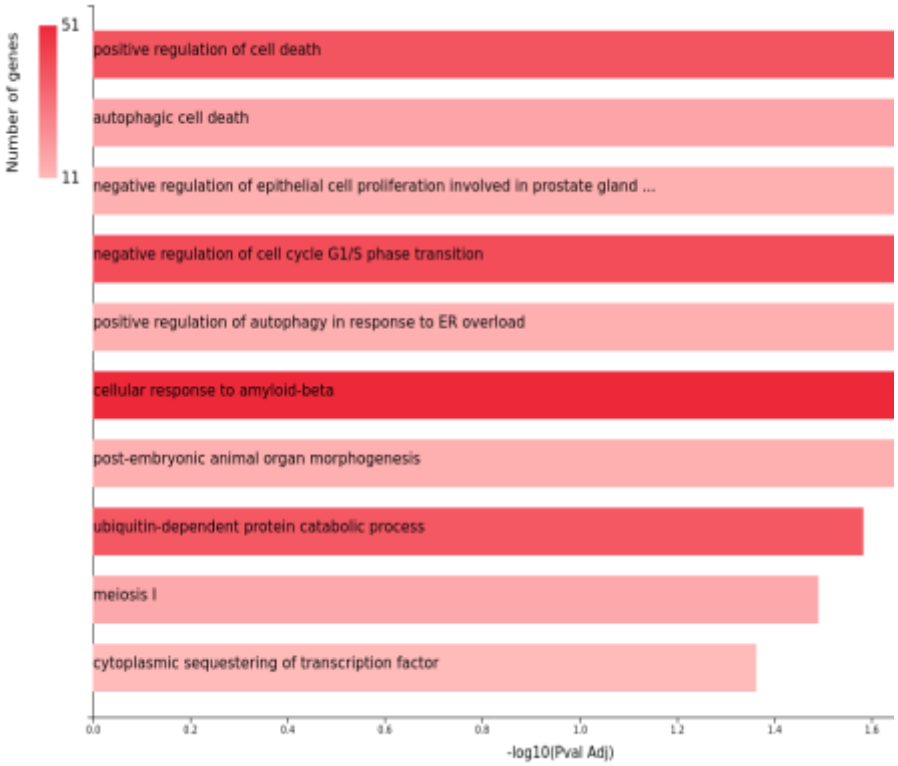

Fig. 2. GO biological processes upregulated by DE miRNAs. Barchart plot of top 10 BP in ccRCC vs. Normal. The x-axis is the $-\log_{10}$ (adjusted *p*-value) while the gene number for each BP is represented on y-axis. It represents negative regulation of cell cycle, cellular response to amyloid beta, ubiquitin-dependent protein catabolism and positive regulation of cell death as significant BP.

Table 3. GO analysis of BP of upregulated DE miRNAs according to GeneCodis4 (p-value < 0.05)

Biological pathway	No. of genes predicted	Total gene count	*P*-value	Important miRNAs
positive regulation of cell death	39	103	6.52E-06	miR-301a-3p, miR-218-5p, miR-143-3p, miR-301b-3p, miR-501-5p, miR-146a-5p
autophagic cell death	17	29	0.0001397	miR-19a-3p, miR-218-5p, miR-155-5p, miR-196a-5p, miR-20a-5p, miR-93-5p
negative regulation of epithelial cell proliferation involved in prostate gland development	14	21	3.92E-06	miR-148a-5p, miR-218-5p, miR-196a-5p, miR-93-5p, miR-378b, miR-155-5p
negative regulation of cell cycle G1/S phase transition	41	114	0.081767	miR-425-5p, miR-34c-5p, miR-218-5p, miR-146a-5p, miR-141-3p, miR-340-5p
positive regulation of autophagy in response to ER overload	14	23	1.87E-05	miR-301b-3p, miR-10b-5p, miR-9-5p, miR-301a-3p, miR-423-3p, miR-32-5p
cellular response to amyloid-beta	51	154	1.68E-05	miR-378a-3p, miR-143-3p, miR-28-5p, miR-501-5p, miR-218-5p, miR-146a-5p
post-embryonic animal organ morphogenesis	14	23	1.87E-05	miR-32-5p, miR-301b-3p, miR-301a-3p, miR-423-3p, miR-10b-5p, miR-9-5p
ubiquitin-dependent protein catabolic process	38	105	3.22E-05	miR-340-5p, miR-143-3p, miR-429, miR-146a-5p, miR-141-3p, miR-10a-3p
meiosis I	16	30	4.47E-05	miR-32-5p, miR-301b-3p, miR-10b-5p, miR-301a-3p, miR-423-3p, miR-9-5p
cytoplasmic sequestering of transcription factor	11	17	7.33E-05	miR-381-3p, miR-378a-3p, miR-196a-5p, miR-141-3p, miR-126-3p, miR-20a-5p

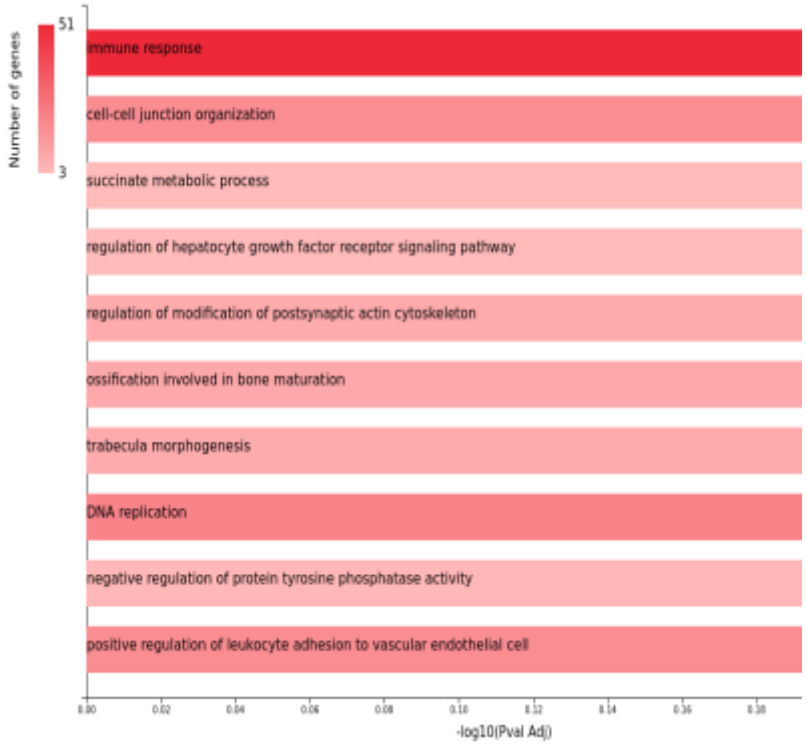

Fig. 3. GO biological processes downregulated by DE miRNAs. Barchart plot of top 10 BP in ccRCC vs. Normal. The x-axis is the $-\log_{10}$ (adjusted *p*-value) while the gene number for each BP is represented on y-axis. It represents positive regulation of leukocyte adhesion to vascular endothelial cells, immune response and DNA replication as significant BP.

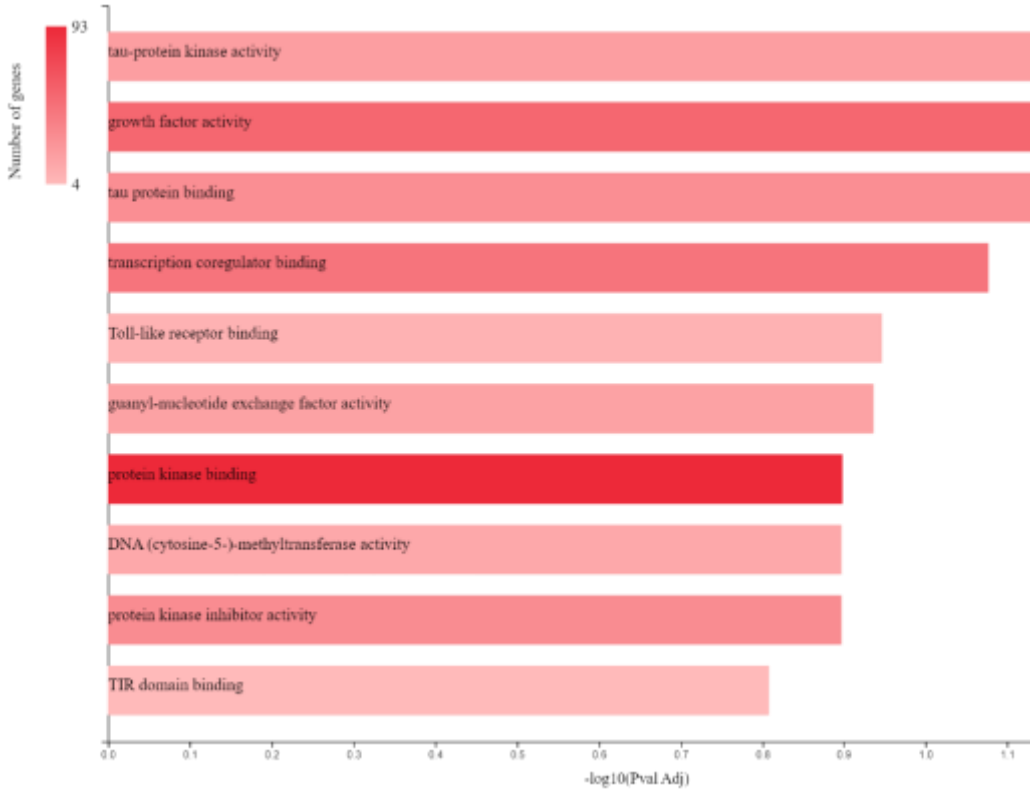

Fig. 4. GO molecular functions upregulated by DE miRNAs. Barchart plot of top 10 MF in ccRCC vs. Normal. The x-axis is the $-\log_{10}$ (adjusted *p*-value) while the gene number for each MF is represented on y-axis. It represents protein kinase binding, growth factor activity, transcription coregulator binding and protein kinase inhibitor activity as significant MF.

Table 4. GO analysis of BP of downregulated DE miRNAs according to GeneCodis4 (p-value < 0.05)

Biological pathway	No. of genes predicted	Total gene count	*P*-value	Important miRNAs
immune response	51	210	0.005923256	miR-150-5p, miR-30d-5p, miR-346, miR-935, miR-31-5p, miR-433-3p
cell-cell junction organization	18	55	0.005478737	miR-29a-3p, miR-30d-5p, miR-424-5p, miR-185-5p, miR-92b-3p, miR-130a-3p
succinate metabolic process	3	3	0.006049045	miR-210-3p, miR-31-3p, miR-29a-3p
regulation of hepatocyte growth factor receptor signaling pathway	3	3	0.006049045	miR-362-3p, miR-122-5p, miR-210-3p
regulation of modification of postsynaptic actin cytoskeleton	8	16	0.003598655	miR-133b, miR-31-5p, miR-185-5p, miR-31-3p, miR-101-3p, miR-490-3p
ossification involved in bone maturation	9	18	0.001978222	miR-133b, miR-214-3p, miR-31-5p, miR-185-5p, miR-31-3p, miR-101-3p
trabecula morphogenesis	8	16	0.003598655	miR-490-3p, miR-31-5p, miR-101-3p, miR-185-5p, miR-31-3p, miR-133b
DNA replication	21	63	0.002014084	miR-424-5p, miR-31-5p, miR-150-5p, miR-185-5p, miR-29c-3p, miR-29a-3p
negative regulation of protein tyrosine phosphatase activity	4	5	0.004662228	miR-424-3p, miR-30d-5p, miR-222-3p, miR-128-3p,
positive regulation of leukocyte adhesion to vascular endothelial cell	18	55	0.005478737	miR-23b-3p, miR-31-3p, miR-31-5p, miR-185-5p, miR-130a-3p, miR-222-3p

Table 5. GO analysis of MF of upregulated DE miRNAs according to GeneCodis4 (p-value < 0.05)

Biological pathway	No. of genes predicted	Total gene count	*P*-value	Important miRNAs
tau-protein kinase activity	21	45	0.054101516	miR-9-5p, miR-340-5p, miR-501-5p, miR-146a-5p, miR-126-3p, miR-616-5p
growth factor activity	55	180	0.067552757	miR-378a-3p, miR-28-5p, miR-146a-5p, miR-218-5p, miR-143-3p, miR-501-5p
tau protein binding	31	84	0.067552757	miR-340-5p, miR-425-5p, miR-34c-5p, miR-501-5p, miR-146a-5p, miR-126-3p
transcription coregulator binding	47	150	0.08390144	miR-378a-3p, miR-126-3p, miR-218-5p, miR-580-3p, miR-141-3p, miR-34c-5p
Toll-like receptor binding	9	14	0.113217276	miR-149-5p, miR-143-3p, miR-19a-3p, miR-146a-5p, miR-155-5p, miR-21-5p
guanyl-nucleotide exchange factor activity	19	45	0.115962	miR-429, miR-501-5p, miR-126-3p, miR-146a-5p, miR-141-3p, miR-10b-5p
protein kinase binding	93	369	0.126475091	miR-501-5p, miR-425-5p, miR-28-5p, miR-378a-3p, miR-218-5p, miR-143-3p
DNA (cytosine-5-)-methyltransferase activity	15	33	0.126922004	miR-20a-5p, miR-143-3p, miR-301b-3p, miR-126-3p, miR-429, miR-30c-5p
protein kinase inhibitor activity	32	95	0.126922004	miR-423-3p, miR-218-5p, miR-196a-5p, miR-28-5p, miR-146a-5p, miR-34c-5p
TIR domain binding	4	4	0.155628884	miR-155-5p, miR-203a-3p, miR-149-5p, miR-21-5p

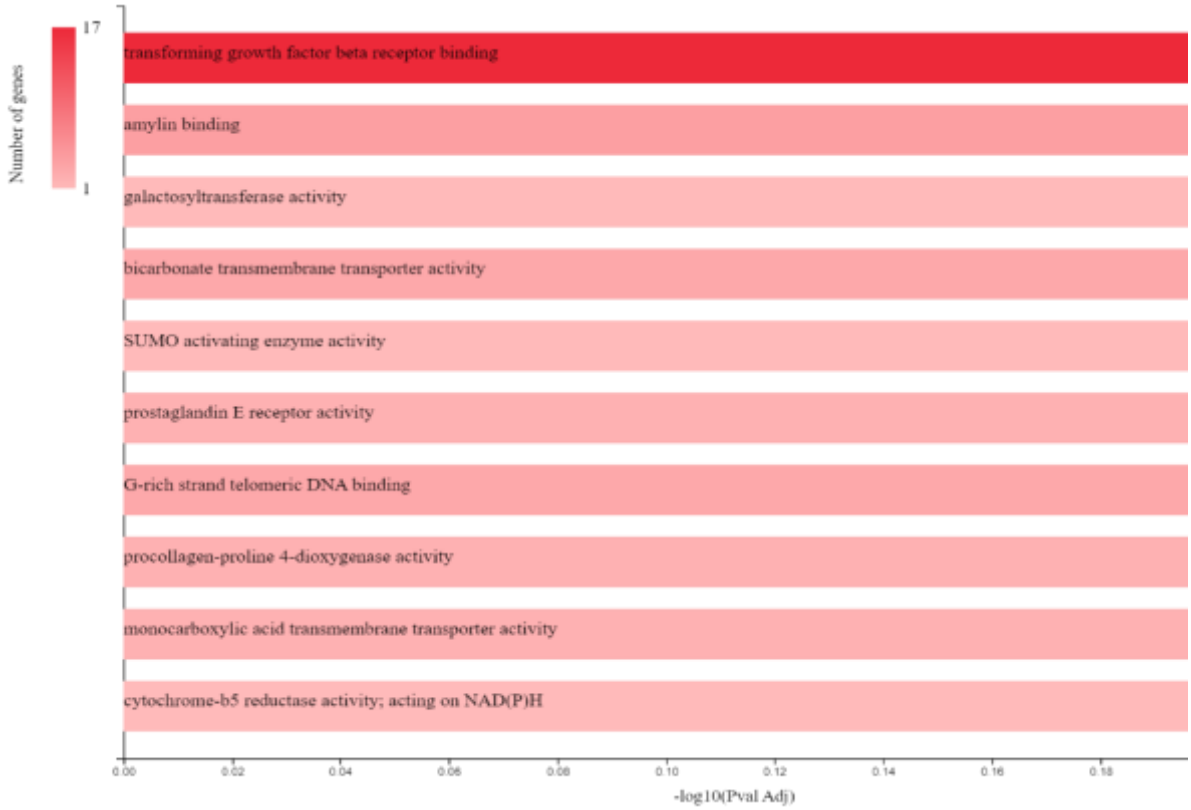

Fig. 5. GO molecular functions downregulated by DE miRNAs. Barchart plot of top 10 MF in ccRCC vs. Normal. The x-axis is the $-\log_{10}$ (adjusted *p*-value) while the gene number for each MF is represented on y-axis. It represents transforming growth factor beta receptor binding as significant MF.

Table 6. GO analysis of MF of downregulated DE miRNAs according to GeneCodis4 (*p*-value < 0.05)

Biological Pathway	Genes predicted	Total gene count	*P*-value	Important miRNAs
transforming growth factor beta receptor binding	17	60	0.032703529	miR-144-3p, miR-92b-3p, miR-424-5p, miR-130a-3p, miR-675-5p, miR-185-5p
amylin binding	4	12	0.162775111	miR-7d-5p, miR-144-3p, miR-130a-3p, miR-101-3p
galactosyltransferase activity	1	1	0.183908046	miR-124-3p
bicarbonate transmembrane transporter activity	3	8	0.167719684	miR-101-3p, miR-433-3p, miR-144-3p
SUMO activating enzyme activity	1	1	0.183908046	miR-133a-3p
prostaglandin E receptor activity	2	4	0.156127606	miR-21-3p, miR-101-3p
G-rich strand telomeric DNA binding	3	7	0.120476441	miR-30a-5p, miR-23a-3p, miR-124-3p
procollagen-proline 4-dioxygenase activity	2	3	0.088615821	miR-210-3p, miR-122-5p
monocarboxylic acid transmembrane transporter activity	2	4	0.156127606	miR-376a-3p, miR-124-3p
cytochrome-b5 reductase activity, acting on NAD(P)H	1	1	0.183908046	miR-214-3p

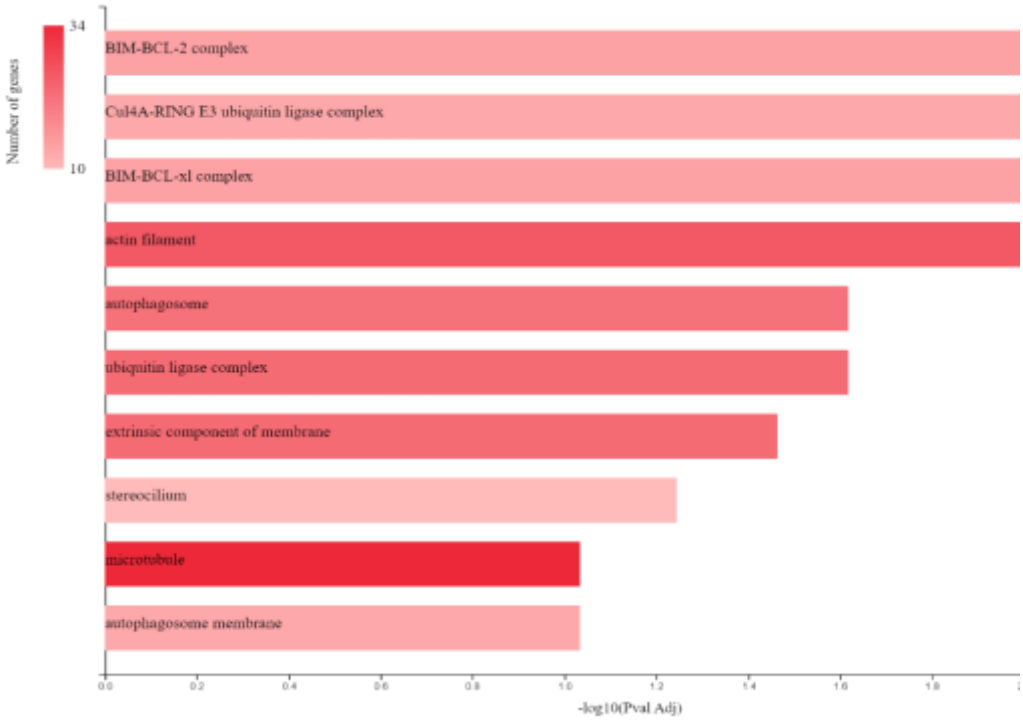

Fig. 6. GO cellular components upregulated by DE miRNAs. Barchart plot of top 10 CC in ccRCC vs. Normal. The x-axis is the – $\log_{10}$ (adjusted *p*-value) while the gene number for each CC is represented on y-axis. It represents microtubule, actin filament, ubiquitin ligase complex and extrinsic component of membrane as significant CC.

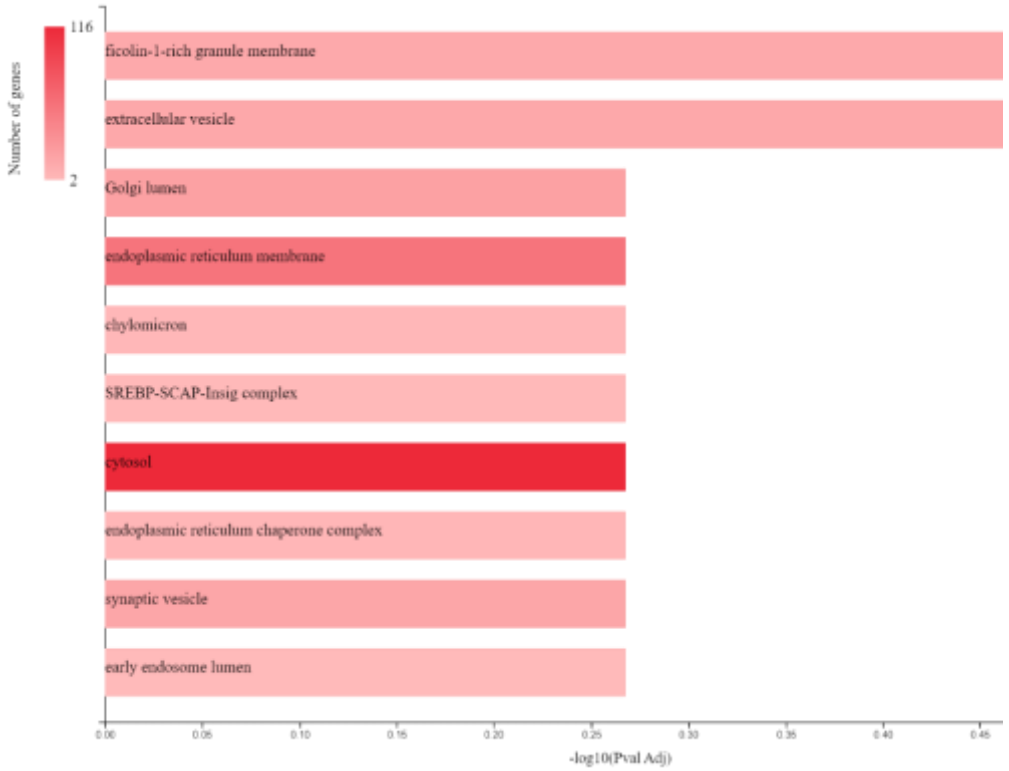

Fig. 7. GO cellular components downregulated by DE miRNAs. Barchart plot of top 10 CC in ccRCC vs. Normal. The x-axis is the –$\log_{10}$ (adjusted *p*-value) while the gene number for each CC is represented on y-axis. It represents cytosol and endoplasmic reticulum membrane as significant CC.

Table 7. GO analysis of CC of upregulated DE miRNAs according to GeneCodis4 (p-value < 0.05)

Biological Pathway	Genes predicted	Total gene count	*P*-value	Important miRNAs
BIM-BCL-2 complex	14	23	0.03734	miR-32-5p, miR-301b-3p, miR-10b-5p, miR-301a-3p, miR-423-3p, miR-9-5p
Cul4A-RING E3 ubiquitin ligase complex	13	20	1.42E-05	miR-452-5p, miR-218-5p, miR-155-5p, miR-196a-5p, miR-9-5p, miR-148a-5p
BIM-BCL-xl complex	14	23	0.03734	miR-32-5p, miR-301b-3p, miR-10b-5p, miR-301a-3p, miR-423-3p, miR-9-5p
actin filament	26	61	3.09E-05	miR-196a-5p, miR-218-5p, miR-141-3p, miR-143-3p, miR-146a-5p, miR-126-3p
autophagosome	22	52	0.000161028	miR-30c-5p, miR-143-3p, miR-9-5p, miR-301a-3p, miR-30e-5p, miR-20a-5p, miR-93-5p
ubiquitin ligase complex	23	55	0.000138849	miR-125a-3p, miR-218-5p, miR-20a-5p, miR-146a-5p, miR-30e-5p, miR-338-5p
extrinsic component of membrane	23	57	0.000268503	miR-10b-5p, miR-146a-5p, miR-196a-5p, miR-301b-3p, miR-301a-3p, miR-423-3p
stereocilium	10	17	0.000507677	miR-96-5p, miR-126-3p, miR-93-5p, miR-301a-3p, miR-493-3p, miR-155-5p
microtubule	34	104	0.001029684	miR-301a-3p, miR-218-5p, miR-34c-5p, miR-143-3p, miR-146a-5p, miR-301b-3p
autophagosome membrane	13	27	0.000947843	miR-155-5p, miR-143-3p, miR-20a-5p, miR-301a-3p, miR-9-5p, miR-93-5p

KEGG pathways analysis of the upregulated and downregulated genes

The DE miRNAs were analyzed using GeneCodis4 for the prediction of KEGG pathways to identify disrupted biological pathways that are affected by the miRNA suppression of target genes. As shown in (Figure 8), the upregulated miRNAs such as miR-378a-3p, miR-218-5p, miR-425-5p, miR-501-5p and miR-141-3p were enriched in T-cell receptor signaling pathway, Yersinia infection, chemokine signaling pathway, shigellosis, Th1 and Th2 cell differentiation and IL-17 signaling pathway (Table 9). This suggests that upregulation of miRNA suppresses these pathways that are mainly involved in immune response and certain infections and results in ccRCC progression. Whereas miRNAs that were downregulated such as miR-487-3p, miR-30d-5p, miR-495-3p, miR-31-5p and miR-185-3p (Table 10) were enriched in renal cell carcinoma, hepatitis B, lipid and atherosclerosis, chronic myeloid leukemia and protein export (Figure 9). The results indicate that the upregulation of genes (ACTR3B, SLC25A5, AKT2, PRRC2A, and SPEN) involved in renal cell carcinoma pathway due to downregulation of miRNA causes cancer development and progression-related functions. This enrichment analysis signifies cancer and cancer related pathways that were previously reported in various carcinomas such as gastric cancer, ovarian cancer, colorectal cancer and breast cancer. This indicates that miRNA regulation of target genes results in disruption of cancer associated biological pathways.

Table 8. GO analysis of CC of downregulated DE miRNAs according to GeneCodis4 (p-value < 0.05)

Biological Pathway	Genes predicted	Total gene count	*P*-value	Important miRNAs
ficolin-1-rich granule membrane	15	36	0.000734962	miR-124-3p, miR-31-5p, miR-29a-3p, miR-185-5p, miR-31-3p, miR-23a-3p
extracellular vesicle	16	39	0.000593082	miR-29a-3p, miR-1908-5p, miR-185-5p, miR-30d-5p, miR-346, miR-29c-3p
Golgi lumen	22	83	0.033962232	miR-130a-3p, miR-31-5p, miR-29c-3p, miR-150-5p, miR-185-5p, miR-487b-3p
endoplasmic reticulum membrane	57	258	0.035215992	miR-433-3p, miR-376b-3p, miR-935, miR-30d-5p, miR-346, miR-31-5p
chylomicron	4	7	0.024409634	miR-485-5p, miR-1908-5p, miR-199a-3p, miR-29a-3p
SREBP-SCAP-Insig complex	3	4	0.021190604	miR-128-3p, miR-185-5p, miR-342-3p
cytosol	116	576	0.00518265	miR-628-3p, miR-376b-3p, miR-30d-5p, miR-487a-3p, miR-1908-5p, miR-346
endoplasmic reticulum chaperone complex	5	10	0.022556154	miR-210-3p, miR-185-5p, miR-495-3p, miR-193a-3p, miR-30a-5p
synaptic vesicle	18	65	0.035768198	miR-144-3p, miR-29c-3p, miR-34a-3p, miR-130a-3p, miR-29a-3p, miR-214-3p
early endosome lumen	2	2	0.033703066	miR-30a-5p, miR-124-3p

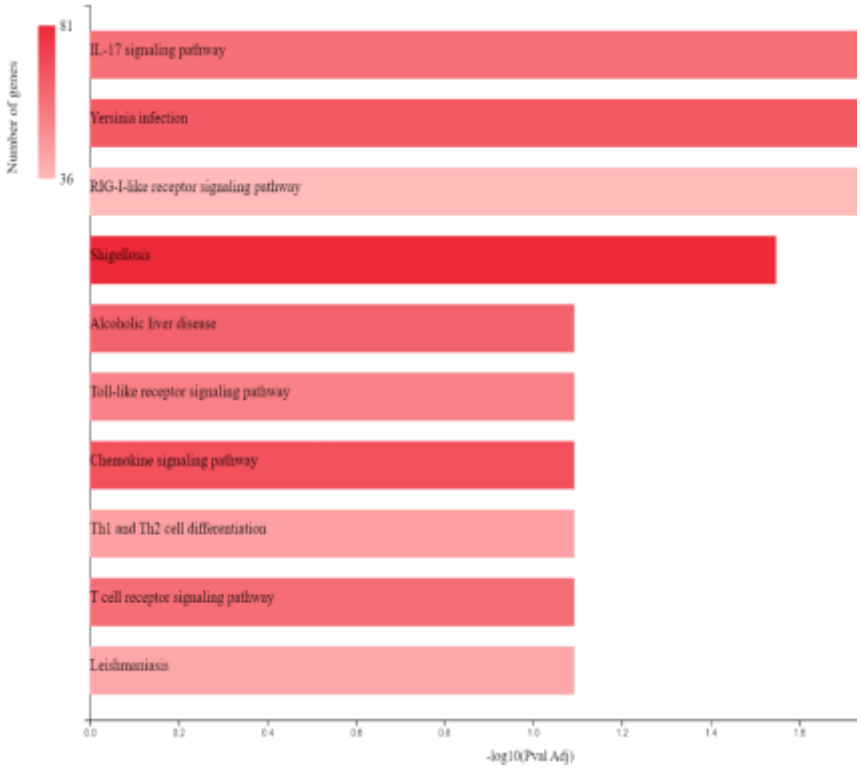

Fig. 8. KEGG pathways analysis of upregulated differentially expressed miRNAs. Barchart plot of top 10 KEGG pathways in ccRCC vs. Normal. The x-axis is the $-\log_{10}$ (adjusted p-value) while the gene number for each pathway is represented on y-axis. It indicates chemokine signaling pathway, shigellosis and T cell receptor signaling pathway as significant pathways.

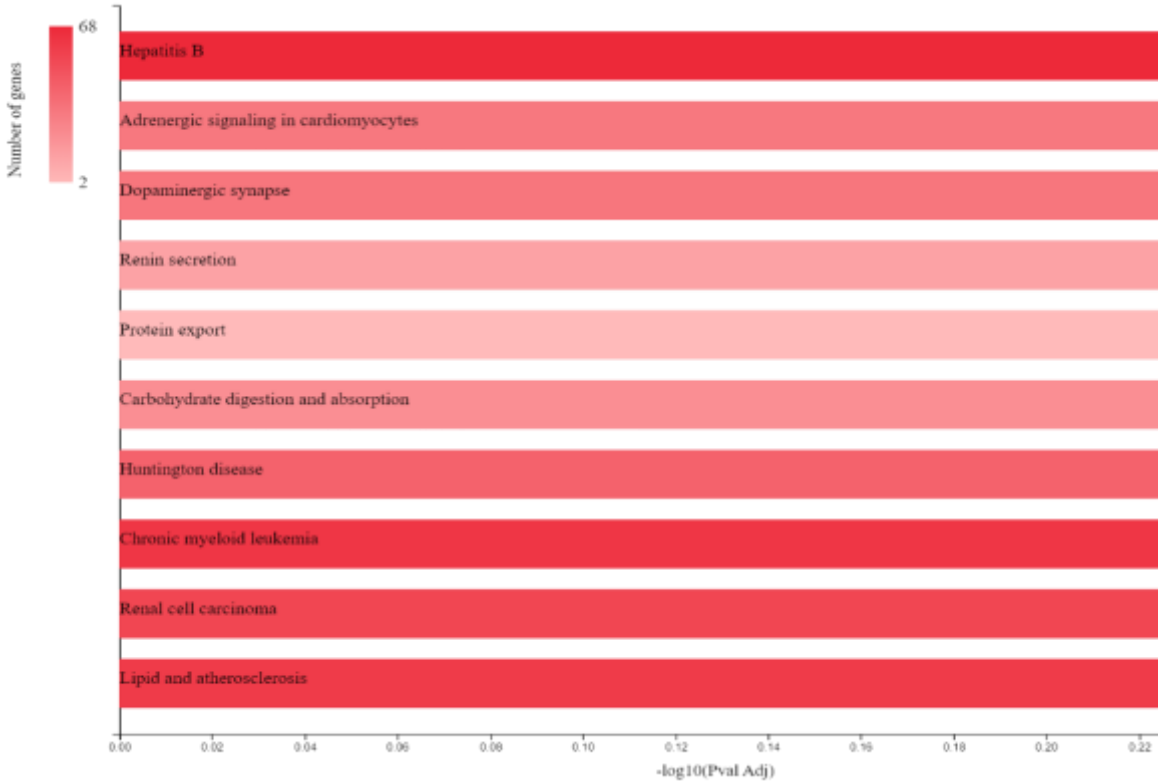

Fig. 9. KEGG pathways analysis of downregulated differentially expressed miRNAs. Barchart plot of top 10 KEGG pathways in ccRCC vs. Normal. The x-axis is the $-\log_{10}$ (adjusted *p*-value) while the gene number for each pathway is represented on y-axis. It indicates hepatitis B, chronic myeloid leukemia and renal cell carcinoma and lipid and atherosclerosis as significant pathways.

Table 9. Pathway prediction for upregulated DE miRNAs according to GeneCodis4 (*p*-value < 0.05)

KEGG Pathway	Genes predicted	Total gene count	*P*-value	Important miRNAs
IL-17 signaling pathway	59	182	3.32E-05	miR-34c-5, miR-378a-3p, miR-218-5p, miR-501-5p, miR-143-3p, miR-28-5p, miR-146a-5p, miR-141-3p
Yersinia infection	66	219	0.000140154	miR-34c-5p, miR-378a-3p, miR-501-5p, miR-218-5p, miR-143-3p, miR-28-5p, miR-146a-5p, miR-141-3p
RIG-I-like receptor signaling pathway	36	97	0.000100927	miR-9-5p, miR-218-5p, miR-143-3p, miR-126-3p, miR-146a-5p, miR-141-3p, miR-30e-5p, miR-196a-5p, miR-10b-5p
Shigellosis	81	291	0.00033127	miR-34c-5p, miR-378a-3p, miR-218-5p, miR-501-5p, miR-143-3p, miR-28-5p, miR-146a-5p, miR-141-3p
Alcoholic liver disease	63	219	0.001179456	miR-340-5p, miR-425-5p, miR-218-5p, miR-146a-5p, miR-143-3p, miR-501-5p, miR-141-3p, miR-34c-5p
Toll-like receptor signaling pathway	54	185	0.002381524	miR-340-5p, miR-378a-3p, miR-218-5p, miR-146a-5p, miR-143-3p, miR-28-5p, miR-141-3p, miR-34c-5p
Chemokine signaling pathway	69	251	0.002602147	miR-34c-5p, miR-378a-3p, miR-218-5p, miR-501-5p, miR-143-3p, miR-28-5p, miR-146a-5p, miR-141-3p

KEGG Pathway	Genes predicted	Total gene count	*P*-value	Important miRNAs
Th1 and Th2 cell differentiation	44	143	0.002267794	miR-340-5p, miR-378a-3p, miR-218-5p, miR-146a-5p, miR-143-3p, miR-28-5p, miR-141-3p, miR-34c-5p
T cell receptor signaling pathway	60	209	0.001845916	miR-34c-5p, miR-378a-3p, miR-218-5p, miR-501-5p, miR-143-3p, miR-28-5p, miR-146a-5p, miR-141-3p
Leishmaniasis	42	134	0.001951695	miR-126-3p, miR-378a-3p, miR-143-3p, miR-141-3p, miR-28-5p, miR-146a-5p, miR-340-5p, miR-10a-3p

Table 10. Pathway prediction for downregulated DE miRNAs according to GeneCodis4 (p-value < 0.05)

KEGG Pathway	Genes predicted	Total gene count	*P*-value	Important miRNAs
Hepatitis B	68	331	0.174897	miR-29c-3p, miR-487a-3p, miR-30d-5p, miR-7b-3p, miR-31-5p, miR-433-3p, miR-185-3p, miR-150-5p, miR-185-5p
Adrenergic signaling in cardiomyocytes	32	151	0.2495	miR-199a-3p, miR-30d-5p, miR-31-5p, miR-150-5p, miR-433-3p, miR-185-3p, miR-185-5p, miR-29c-3p, miR-29a-3p
Dopaminergic synapse	33	140	0.076701	miR-129-1-3p, miR-30d-5p, miR-346, miR-185-3p, miR-31-5p, miR-433-3p, miR-150-5p, miR-185-5p, miR-29c-3p
Renin secretion	13	54	0.204949	miR-371a-3p, miR-30d-5p, miR-433-3p, miR-29a-3p, miR-150-5p, miR-424-5p, miR-133a-3p, miR-23b-3p, miR-222-3p
Protein export	2	4	0.165059	miR-30a-5p, miR-495-3p
Carbohydrate digestion and absorption	22	84	0.052359	miR-495-3p, miR-487a-3p, miR-30d-5p, miR-29a-3p, miR-185-3p, miR-29c-3p, miR-199a-3p, miR-133a-3p, miR-23a-3p
Huntington disease	42	177	0.039429	miR-31-3p, miR-376b-3p, miR-30d-5p, miR-150-5p, miR-31-5p, miR-433-3p, let-7b-3p, miR-29c-3p, miR-424-5p
Chronic myeloid leukemia	62	302	0.201436	miR-487b-3p, miR-487a-3p, miR-30d-5p, miR-150-5p, miR-31-5p, miR-433-3p, miR-185-3p, miR-185-5p, miR-29c-3p
Renal cell carcinoma	55	237	0.024518	miR-487b-3p, miR-487a-3p, miR-30d-5p, miR-31-5p, miR-150-5p, miR-433-3p, miR-185-3p, miR-185-5p, miR-29c-3p
Lipid and atherosclerosis	60	297	0.265945	miR-185-5p, miR-487a-3p, miR-30d-5p, miR-433-3p, miR-346, miR-31-5p, let-7b-3p, miR-185-3p, miR-150-5p

DISCUSSION

Generally, ccRCC accounts for 85 % of all primary kidney cancers. Understanding the fundamental mechanisms is important for identifying the disease prognosis and potential drug targets for ccRCC. RNASeq is proved to be a quantitative tool for DEA that identifies miRNA expression level with greater accuracy and higher efficiency to provide insights on putative therapeutic targets. This study identifies 2656 DE miRNAs, and among them 229 were upregulated and 302 were downregulated. The identified upregulated miRNAs include

miR-140-5p, miR-126-3p, miR-28-5p, miR-20a-5p, miR-671-5p, miR-186-5p, miR-627-5p, miR-338-5p, miR-30e-3p and miR-148b-5p, whereas the downregulated miRNAs include miR-424-3p, miR-107, miR-23b-5p, miR-499a-5p, miR-23a-3p, miR-128-3p, miR-7977, miR-29c-3p, miR-5100 and miR-4454. Functional enrichment analysis indicated that these miRNAs were mostly involved in the dysregulation of biological pathways and process such as negative regulation of cell cycle G1/S phase transition, immune response, DNA replication and positive regulation of cell death.

In this present study, it was found that miR-140-5p upregulation causes KLF9 suppression and KCNQ1 downregulation, which plays crucial role in cellular electric signals transmission. This serves as a foundation in ccRCC progression and metastasis due to dysregulated signaling pathway [19]. Similarly, the upregulation of miR-126-3p and miR-20a-5p is involved in disruption of apoptosis by downregulating PI3k (phosphatidylinositol 3-kinase) pathway and CXCL8 expression respectively. This leads to decline in immune cells recruitment which results in suppressed apoptosis and increased growth and proliferation [20], [21]. Upregulated miR-28-5p and miR-671-5p inhibits Mad2 translation and anaphase promoting complex (APC), resulting in chromosomal instability and increased metastasis due to anaphase progression inhibition until correct alignment of spindle microtubules [22], [23]. Higher levels of miR-186-5p in ccRCC individuals dysregulates glucose transporter 1 (GLUT-1), which is responsible for basal glucose uptake to sustain cellular respiration. A disrupted expression of GLUT-1 results in disturbed cellular metabolism, a significant hallmark of cancer [24]. In colorectal neoplasms it was found that miR-627-5p serum levels were increased that leads to NUP160 suppression resulting in cell proliferation inhibition and stimulation of autophagy and apoptosis [25]. It has been reported that colorectal cancer metastasis is promoted by increased miR-338-5p levels by inhibiting autophagy pathway mediated by phosphatidylinositol 3-kinase, catalytic subunit type 3 (PIK3C3) [26]. Upregulated miR-30e-3p has been found in primary tumors of breast cancer patients and is linked to epithelial-mesenchymal transition (EMT) induction, which is a prerequisite for tumor cell distribution [27]. It has been reported that upregulated miR-148b-5p suppresses ATPase inhibitory factor 1 (ATPIF-1) that prevents oxidative phosphorylation (OP) and promotes aerobic glycolysis. This leads to increased OP that provides energy to tumor cells [28]. Through literature, it was found that miR-424-3p downregulation leads to increased invasiveness in prostate cancer due to high expression of CTLA-4 that functions as an immune checkpoint and downregulates immune system [29]. Downregulation of miR-107 and miR-29c-3p causes upregulation of KCNQ1OT1 and MAPK signaling pathway respectively, which results in uncontrolled cell proliferation and increased growth promoting pathways in hepatocellular carcinoma (HCC), gallbladder cancer, colon cancer and breast cancer [30], [31]. A downregulated miR-23b-5p and miR-23a-3p causes FOXM1 and AKT1 upregulation that promotes various oncogenic phenotypes such as cell proliferation, cancer stem cell properties and invasion and metastasis in ovarian cancer and HCC [32]–[34]. It has been reported that downregulated miR-499a-5p results in non-small cell lung cancer cell lines and tissues and promotes lung cancer cells proliferation and colony formation, and induce S-phase of cell cycle [35]. MiR-128-3p downregulation causes ZEB1 overexpression that leads to human esophageal squamous-cell carcinoma (ESCC) invasiveness and metastasis by increased cell proliferation [36]. Lower expression of miR-4454 promotes tyrosine kinase (TK) function in ccRCC patients, which is an essential mediator of signal transduction process. Upregulated TKs results in increased cell proliferation and migration in ccRCC [37]. Moreover downregulation of miR-5100 leads to upregulated DUSP16 which leads to tumorigenesis by preventing senescence in human liver cancer cells [38].

KEGG pathway enrichment analysis showed that upregulated DE miRNAs were significantly associated with T cell receptor signaling pathway, shigellosis, chemokine signaling pathway, while downregulated DE miRNAs were involved in renal cell carcinoma, hepatitis B and chronic myeloid leukemia. In this study it was found that upregulated miR-

378a-3p dysregulates pathways involved in shigellosis. It has been reported that shigella induces apoptosis via mitochondrial related cell death, but its downregulation leads to cancer progression due to impaired apoptosis and increased cell differentiation [39]. Furthermore, miR-218-5p upregulation inhibits LRIG1, a transmembrane protein, in breast cancer. This protein interacts with TK of epidermal growth factor receptors (EGFR) and its suppression promotes EGFR expression that leads to increased cell migration and differentiation in breast cancer [40]. In addition, upregulation of miR-143-3p suppresses VASH1, involved in cellular movement and negative regulation of angiogenesis and proteolysis. This results in higher cell migration and increased angiogenesis that supplies blood to tumor cells to grow [41]. Furthermore, downregulation of miR-487a-3p upregulates protein phosphatase 1A (PPM1A) which in turn upregulates MAP kinases that are responsible for cell motility, differentiation and viability in oral squamous cell carcinoma [42]. It has been reported that miR-30d-5p downregulation promotes GRP78 expression that is responsible for proliferation and anti-apoptosis of ccRCC cells. Therefore miR-30d-5p downregulation demonstrates oncogenic activities [43]. Moreover downregulation of miR-185-3p upregulates WNT2B which is involved in stem cell renewal and maintenance. This leads to increased invasion and metastasis resulting in tumor progression in nasopharyngeal carcinoma [44].

Thus, this study provides key insights into the up and down regulated miRNAs and their effects on their target genes. Moreover, a novel set of five miRNAs (miR-627-5p, miR-30e-3p, miR-424-3p, miR-23b-5p, miR-218-5p) have been identified that were not reported previously and are involved in the ccRCC progression and development.

CONCLUSION

The miRNA dysregulation imparts a significant influence on development of multiple human cancers such as renal cancer, breast cancer, hepatocellular carcinoma, pancreatic cancer, ovarian cancer, colorectal cancer, nasopharyngeal carcinoma and prostate cancer. This study identified 2656 DE miRNAs and among them 229 were upregulated and 302 were downregulated. It was found that five miRNAs (miR-140-5p, miR-671-5p, miR-186-5p, miR-4454, miR-30d-5p) were significantly associated with ccRCC development and progression. This study provides key insights into the effects caused by dysregulated miRNAs on their target gene. It was found that overexpression of miR-140-5p dysregulates a transcriptional regulator, KLF9. This results in disrupted signaling pathways in ccRCC cells due to suppressed electric signal transmission leading to uncontrolled cell growth. Furthermore, it was found that upregulated miR-671-5p regulates ccRCC metastasis by targeting anaphase promoting complex, which promotes cell migration and polarity through Wnt signaling pathway. Moreover miR-186-5p upregulation, downregulates glucose transporter, GLUT-1, which leads to disrupted cell metabolism. Downregulation of miR-4454 mediates signal transduction by tyrosine kinase overexpression leading to increased cell proliferation, migration, differentiation and metabolism. It was also found that downregulated miR-30d-5p result in GRP78 overexpression, which promotes enhanced ccRCC cells proliferation and decreased apoptosis. However, a novel set (miR-627-5p, miR-30e-3p, miR-424-3p, miR-23b-5p, miR-218-5p) of miRNAs that have not been reported for ccRCC previously but found in multiple human carcinomas, have been identified in this study that suggest the deregulation of crucial genes suggesting ccRCC development and progression. In summary, these known and novel sets of DE miRNAs are suggested as important and deregulated miRNAs for ccRCC.

REFERENCES

1 Tahbaz R., Schmid M., Merseburger A.S. Prevention of kidney cancer incidence and recurrence: lifestyle, medication and nutrition. *Curr. Opin. Urol*. 2018. V. 28. No. 1. P. 62–79. doi: 10.1097/MOU.0000000000000454

2 Gomella P.T., Linehan W.M., Ball M.W. Precision surgery and kidney cancer: knowledge of genetic alterations influences surgical management. *Genes*. 2021. V. 12. No. 2. Article No. 261. doi: 10.3390/genes12020261

3 Capitanio U., Bensalah K., Bex A., Boorjian S.A., Bray F., Coleman J., Gore J.L., Sun M., Wood C., Russo P. Epidemiology of renal cell carcinoma. *European Urology*. 2019. V. 75. No. 1. P. 74–84. doi: 10.1016/j.eururo.2018.08.036

4 Linehan W.M., Schmidt L.S., Crooks D.R., Wei D., Srinivasan R., Lang M., Ricketts C.J. The Metabolic Basis of Kidney CancerThe Metabolic Basis of Kidney Cancer. *Cancer Discovery*. 2019. V. 9. No. 8. P. 1006–1021. doi: 10.1158/2159-8290.CD-18-1354

5 Sung H., Ferlay J., Siegel R.L., Laversanne M., Soerjomataram I., Jemal A., Bray F. Global cancer statistics 2020: GLOBOCAN estimates of incidence and mortality worldwide for 36 cancers in 185 countries. *CA: A Cancer Journal for Clinicians*. 2021. V. 71. No. 3. P. 209–249. doi: 10.3322/caac.21660

6 Wolf M.M., Kimryn Rathmell W., Beckermann K.E. Modeling clear cell renal cell carcinoma and therapeutic implications. *Oncogene*. 2020. V. 39. P. 3413–3426. doi: 10.1038/s41388-020-1234-3

7 Hsieh J.J., Purdue M.P., Signoretti S., Swanton C., Albiges L., Schmidinger M., Heng D.Y, Larkin J., Ficarra V. Renal cell carcinoma. *Nat. Rev. Dis. Primers*. 2017. V. 3. Article No. 17009. doi: 10.1038/nrdp.2017.9

8 Eliasson L., Regazzi R. Micro(RNA) management and mismanagement of the islet. *Journal of Molecular Biology*. 2020. V. 432. No. 5. P. 1419–1428. doi: 10.1016/j.jmb.2019.09.017

9 Budakoti M., Panwar A.S., Molpa D., Singh R.K., Büsselberg D., Mishra A.P., Coutinho H.D., Nigam M. Micro-RNA: The darkhorse of cancer. *Cellular Signalling*. 2021. V. 83. Article No. 109995. doi: 10.1016/j.cellsig.2021.109995

10 Weidle U.H., Nopora A. Clear Cell Renal Carcinoma: MicroRNAs With Efficacy in Preclinical *In Vivo* Models. *Cancer Genomics & Proteomics*. 2021. V. 18. No. 3 Suppl. P. 349–368. doi: 10.21873/cgp.20265

11 Huang Y.X., Nie X.G., Li G.D., Fan D.S., Song L.L., Zhang X.L. Downregulation of microRNA-182 inhibits cell viability, invasion and angiogenesis in retinoblastoma through inhibition of the PI3K/AKT pathway and CADM2 upregulation. *International Journal of Oncology*. 2018. V. 53. No. 6. P. 2615–2626. doi: 10.3892/ijo.2018.4587

12 Ullah R., Naz A., Akram H.S., Ullah Z., Tariq M., Mithani A., Faisal A. Transcriptomic analysis reveals differential gene expression, alternative splicing, and novel exons during mouse trophoblast stem cell differentiation. *Stem Cell Research & Therapy*. 2020. V. 11. Article No. 342. doi: 10.1186/s13287-020-01848-8

13 Rostovskaya M., Andrews S., Reik W., Rugg-Gunn P.J. Amniogenesis occurs in two independent waves in primates. *Cell Stem Cell*. 2022. V. 29. No. 5. P. 744–759. doi: 10.1016/j.stem.2022.03.014

14 Chen S.C., Kuo P.L. Bone metastasis from renal cell carcinoma. *International Journal of Molecular Sciences*. 2016. V. 17. No. 6. Article No. 987. doi: 10.3390/ijms17060987

15 Liu F., Tang Y., Guo Q., Chen J. Identification and characterization of microRNAs in phloem and xylem from ramie (Boehmeria nivea). *Molecular Biology Reports*. 2020. V. 47. P. 1013–1020. doi: 10.1007/s11033-019-05193-9

16 Kozomara A., Birgaoanu M., Griffiths-Jones S. miRBase: from microRNA sequences to function. *Nucleic Acids Research*. 2019. V. 47. No. D1. P. D155–D162. doi: 10.1093/nar/gky1141

17 Love M.I., Huber W., Anders S. Moderated estimation of fold change and dispersion for RNA-seq data with DESeq2. *Genome Biology*. 2014. V. 15. Article No. 550. doi: 10.1186/s13059-014-0550-8

18 Garcia-Moreno A., López-Domínguez R., Villatoro-García J.A., Ramirez-Mena A., Aparicio-Puerta E., Hackenberg M., Pascual-Montano A., Carmona-Saez P. Functional Enrichment Analysis of Regulatory Elements. *Biomedicines*. 2022. V. 10. No. 3. Article No. 590. doi: 10.3390/biomedicines10030590

19 Huang C., Li J., Zhang X., Xiong T., Ye J., Yu J., Gui Y. The miR-140-5p/KLF9/KCNQ1 axis promotes the progression of renal cell carcinoma. *The FASEB Journal*. 2020. V. 34. P. 10623–10639. doi: 10.1096/fj.202000088RR

20 Bai Y., Li H., Dong J. Up-regulation of miR-20a weakens inflammation and apoptosis in high-glucose-induced renal tubular cell mediating diabetic kidney disease by repressing CXCL8 expression. *Archives of Physiology and Biochemistry*. 2022. V. 128. No 6. P. 1603–1610. doi: 10.1080/13813455.2020.1785506

21 Carlsson J., Christiansen J., Davidsson S., Giunchi F., Fiorentino M., Sundqvist P. The potential role of miR-126, miR-21 and miR-10b as prognostic biomarkers in renal cell carcinoma. *Oncology Letters*. 2019. V. 17. No. 5. P. 4566–4574. doi: 10.3892/ol.2019.10142

22 Chi X.G., Meng X.X., Ding D.L., Xuan X.H., Chen Y.Z., Cai Q., Wang A. HMGA1-mediated miR-671-5p targets APC to promote metastasis of clear cell renal cell carcinoma through Wnt signaling. *Neoplasma*. 2020. V. 67. No. 1. P. 46–53.

23 Hell M.P., Thoma C.R., Fankhauser N., Christinat Y., Weber T.C., Krek W. miR-28-5p Promotes Chromosomal Instability in VHL-Associated Cancers by Inhibiting Mad2 TranslationpVHL Controls Aneuploidy via miR-28-5p. *Cancer Research*. 2014. V. 74. No. 9. P. 2432–2443. doi: 10.1158/0008-5472.CAN-13-2041

24 Morais M., Dias F., Nogueira I., Leão A., Gonçalves N., Araújo L., Granja S., Baltazar F., Teixeira A.L., Medeiros R. Cancer cells' metabolism dynamics in renal cell carcinoma patients' outcome: influence of GLUT-1-Related hsa-miR-144 and hsa-miR-186. *Cancers.* 2021. V. 13. No. 7. Article No. 1733. doi: 10.3390/cancers13071733

25 Wang P., Zhao F., Nie X., Liu J., Yu Z. Knockdown of NUP160 inhibits cell proliferation, induces apoptosis, autophagy and cell migration, and alters the expression and localization of podocyte associated molecules in mouse podocytes. *Gene.* 2018. V. 664. P. 12–21. doi: 10.1016/j.gene.2018.04.067

26 Chu C.A., Lee C.T., Lee J.C., Wang Y.W., Huang C.T., Lan S.H., Lin P.C., Lin B.W., Tian Y.F., Liu H.S. et al. MiR-338-5p promotes metastasis of colorectal cancer by inhibition of phosphatidylinositol 3-kinase, catalytic subunit type 3-mediated autophagy pathway. *eBioMedicine*. 2019. V. 43. P. 270–281. doi: 10.1016/j.ebiom.2019.04.010

27 Block I., Burton M., Sørensen K.P., Andersen L., Larsen M.J., Bak M., Cold S., Thomassen M., Tan Q., Kruse T.A. Association of miR-548c-5p, miR-7-5p, miR-210-3p, miR-128-3p with recurrence in systemically untreated breast cancer. *Oncotarget*. 2018. V. 9. P. 9030–9042. doi: 10.18632/oncotarget.24088

28 Zhang Y., Huo W., Sun L., Wu J., Zhang C., Wang H., Wang B., Wei J., Qu C., Cao H. et al. Targeting miR-148b-5p Inhibits Immunity Microenvironment and Gastric Cancer

Progression. *Frontiers in Immunology*. 2021. V. 12. Article No. 590447. doi: 10.3389/fimmu.2021.590447

29 Richardsen E., Andersen S., Al-Saad S., Rakaee M., Nordby Y., Pedersen M.I., Ness N., Ingebriktsen L.M., Fassina A., Tasken K.A. et al. Low expression of miR-424-3p is highly correlated with clinical failure in prostate cancer. *Scientific Reports*. 2019. V. 9. Article No. 10662. doi: 10.1038/s41598-019-47234-0

30 Fang R., Huang Y., Xie J., Zhang J., Ji X. Downregulation of miR-29c-3p is associated with a poor prognosis in patients with laryngeal squamous cell carcinoma. *Diagnostic Pathology*. 2019. V. 14. Article No. 109. doi: 10.1186/s13000-019-0893-2

31 Wu Y., Bi Q.J., Han R., Zhang Y. Long noncoding RNA KCNQ1OT1 is correlated with human breast cancer cell development through inverse regulation of hsa-miR-107. *Biochemistry and Cell Biology*. 2020. V. 98. No. 3. P. 338–344. doi: 10.1139/bcb-2019-0271

32 He R.Q., Wu P.R., Xiang X.L., Yang X., Liang H.W., Qiu X.H., Yang L.H., Peng Z.G., Chen G. Downregulated miR-23b-3p expression acts as a predictor of hepatocellular carcinoma progression: A study based on public data and RT-qPCR verification. *International Journal of Molecular Medicine*. 2018. V. 41. No. 5. P. 2813–2831. doi: 10.3892/ijmm.2018.3513

33 Liu C., Barger C.J., Karpf A.R. Foxm1: A multifunctional oncoprotein and emerging therapeutic target in ovarian cancer. *Cancers*. 2021. V. 13. No. 12. Article No. 3065. doi: 10.3390/cancers13123065

34 Yang X., Yang S., Song J., Yang W., Ji Y., Zhang F., Rao J. Dysregulation of miR-23b-5p promotes cell proliferation via targeting FOXM1 in hepatocellular carcinoma. *Cell Death Discovery*. 2021. V. 7. Article No. 47. doi: 10.1038/s41420-021-00440-0

35 Zhao L., Jiang P., Zheng H., Chen P., Yang M. Downregulation of miR-499a-5p predicts a poor prognosis of patients with non-small cell lung cancer and restrains the tumorigenesis by targeting fibroblast growth factor 9. *Technology in Cancer Research & Treatment*. 2020. V. 19. Article No. 1533033820957001. doi: 10.1177/1533033820957001

36 Zhao L., Li R., Xu S., Li Y., Zhao P., Dong W., Liu Z., Zhao Q., Tan B. Tumor suppressor miR-128-3p inhibits metastasis and epithelial–mesenchymal transition by targeting ZEB1 in esophageal squamous-cell cancer. *Acta Biochimica et Biophysica Sinica*. 2018. V. 50. No. 2. P. 171–180. doi: 10.1093/abbs/gmx132

37 Lukamowicz-Rajska M., Mittmann C., Prummer M., Zhong Q., Bedke J., Hennenlotter J., Stenzl A., Mischo A., Bihr S., Schmidinger M. et al. MiR-99b-5p expression and response to tyrosine kinase inhibitor treatment in clear cell renal cell carcinoma patients. *Oncotarget*. 2016. V. 7. P. 78433–78447. doi: 10.18632/oncotarget.12618

38 Zhang H., Zheng H., Mu W., He Z., Yang B., Ji Y., Hui L. DUSP 16 ablation arrests the cell cycle and induces cellular senescence. *The FEBS Journal*. 2015. V. 282. No. 23. P. 4580–4594. doi: 10.1111/febs.13518

39 Wei X., Li H., Zhang B., Li C., Dong D., Lan X., Huang Y., Bai Y., Lin F., Zhao X. et al. miR-378a-3p promotes differentiation and inhibits proliferation of myoblasts by targeting HDAC4 in skeletal muscle development. *RNA Biology*. 2016. V. 13. No. 12. P. 1300-1309. doi: 10.1080/15476286.2016.1239008

40 Qian M., Xu H., Song H., Xi H., Fang L. MiR-218-5p promotes breast cancer progression via LRIG1: preprint. *Research Square*. 2021. doi: 10.21203/rs.3.rs-203193/v1

41 Wang H., Deng Q., Lv Z., Ling Y., Hou X., Chen Z., Dinglin X., Ma S., Li D., Wu Y. et al. N6-methyladenosine induced miR-143-3p promotes the brain metastasis of lung cancer via regulation of VASH1. *Molecular Cancer*. 2019. V. 18. Article No. 181. doi: 10.1186/s12943-019-1108-x

42 Wang L., Ge S., Zhou F. MicroRNA-487a-3p inhibits the growth and invasiveness of oral squamous cell carcinoma by targeting PPM1A. *Bioengineered.* 2021. V. 12. No. 1. P. 937–947. doi: 10.1080/21655979.2021.1884396

43 Wang C., Cai L., Liu J., Wang G., Li H., Wang X., Xu W., Ren M., Feng L., Liu P. et al. MicroRNA-30a-5p inhibits the growth of renal cell carcinoma by modulating GRP78 expression. *Cellular Physiology and Biochemistry*. 2017. V. 43. No. 6. P. 2405–2419. doi: 10.1159/000484394

44 Liu C., Li G., Ren S., Su Z., Wang Y., Tian Y., Liu Y., Qiu Y. miR-185-3p regulates the invasion and metastasis of nasopharyngeal carcinoma by targeting WNT2B *in vitro*. *Oncology Letters*. 2017. V. 13. No. 4. P. 2631-2636. doi: 10.3892/ol.2017.5778

Received 07.10.2022.
Revised 17.11.2022.
Published 25.11.2022.